# A Magneto-statics Inspired Transform for Structure Representation and Analysis of Digital Images

XIAO-DONG ZHUANG[1] and NIKOS E. MASTORAKIS[1,2]
[1] WSEAS Headquarters, Agiou Ioannou Theologou 17-23, 15773, Zografou, Athens, GREECE
xzhuang@worldses.org
[2] Department of Computer Science, Military Institutions of University Education, Hellenic Naval Academy, Terma Hatzikyriakou, 18539, Piraeus, GREECE
mastor@wseas.org http://www.wseas.org/mastorakis

*Abstract:* - Physical-field inspired methodology has become a new branch in image processing techniques. In this paper, a novel image transform is proposed imitating the source reverse of magneto-static field. The image is taken as a vertical magnetic field, and its curl is estimated as the virtual source of the field for image structure representation and analysis. The restoration from the virtual source to the image is also investigated, based on which a method of image estimation and restoration from its gradient field is proposed. The experimental results indicate that the proposed curl source reverse provides effective image structure representation, which can be exploited in further image processing tasks.

*Key-Words:* - Image transform, curl source reverse, magneto-static, image structure, image restoration

## 1 Introduction

In digital image processing, the image transform is the basis for many real world applications, such as the widely applied classic Fourier transform and the popular Wavelet transform [1,2,3]. The emergence of new transform techniques improves the development of image processing with support for real world applications. In recent years, the emergence of physical field inspired methods has attracted more and more research and achieved good results in image processing tasks such as ear recognition, image segmentation, corner detection, etc [4-11].

Generally speaking, in physics the field is determined by the source distribution [12,13]. Therefore, the field can always reflect some characteristics of the source, which is the foundation of the effectiveness of the field inspired methods. Currently, these methods focus on the direction where the image is just taken as the virtual source of the field [4-11]. Then the processing and analysis are carried out in the virtual field generated by the image imitating the electro-static or magneto-static field.

The physical-field inspired methods gradually form a new trend in image processing based on their successful applications. The effectiveness of the virtual fields in image processing tasks inspires a novel idea of field source reverse in our research. Previous field-based methods usually take the image as the source to produce the virtual field. However, the novel idea presented in this paper takes the image as the virtual field and investigates the properties of the virtual curl source with a reverse method inspired by the magneto-static field.

Based on the above novel idea, an image transform is presented, which is different from previous field inspired methods. The curl source reverse is proposed imitating the reverse of the magnetic field. The image is taken as a virtual magneto-static field, and the virtual curl source is reversed from the image as an efficient structure representation for further processing tasks. The analysis and experimental results indicate that the proposed transform can reveal structural characteristics of images. Moreover, the opposite transform from the virtual curl source to the original image is also investigated, based on which a method of estimate and restore the original image from its gradient field is presented. The effectiveness of the restoration method is also proved experimentally.

## 2 The Curl Source Reverse for Digital Images

### 2.1 The Relationship between the Magnetic Field and the Field Source

In physics, moving charges generate magnetic field in the space. Thus the moving charges (i.e. the current) can be conceptually regarded as the source of the magnetic field. On the other hand, if the magnetic field is known, the field source of current density can be reversed according to the Ampere's law in differential form [12,13]:

$$\nabla \times \vec{B} = \mu_0 \cdot \vec{J} \tag{1}$$

where $\vec{B}$ is the magnetic induction; $\vec{J}$ is the current density (i.e. the field source distribution); $\mu_0$ is the permeability constant; $\nabla$ is the Hamiltonian operator:

$$\nabla = \frac{\partial}{\partial x}\vec{i} + \frac{\partial}{\partial y}\vec{j} + \frac{\partial}{\partial z}\vec{k} \tag{2}$$

The operator $\nabla$ means the cross product of two vectors. The operation of $\nabla\times$ obtains the curl of the vector field $\vec{B}$, i.e. the source distribution $\vec{J}$ has direct relationship to the curl of $\vec{B}$. Therefore, the reverse from the magnetic field to the source is as following:

$$\vec{J} = \frac{\nabla \times \vec{B}}{\mu_0} \tag{3}$$

Because the source reflects underlying structural feature of the field, in this paper a transform from the image to the virtual curl source is proposed for image structure representation in the next section.

## 2.2 The Virtual Curl Source Reverse

In physics, the field is determined by the source distribution. Therefore, the field source can be a compact representation of the field and may reveal structural characteristics of the field, which can be exploited in image transform and analysis.

In this paper, a novel image transform is presented imitating the source reverse of the magnetic field. Because the source distribution of magnetic field is its curl, the transform is named the curl source reverse.

The image $f(x,y)$ itself is a scalar distribution in the 2-D domain. To get the virtual curl source of the image, each image pixel is represented by a vector $\vec{I}(x,y)$, which comes outward from the 2-D plane. Moreover, the vector representing a pixel is at a right angle to the 2-D plane and its magnitude is defined as the gray-scale value of that pixel:

$$\vec{I}(x,y) = f(x,y) \cdot \vec{k} \tag{4}$$

With such definition, the image $f$ is represented by a vertical vector field $\vec{I}$. A simple example of the vector field representing a small image of the size 3×3 is shown in Fig. 1.

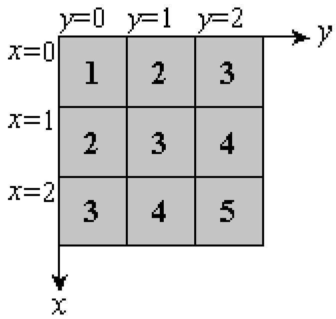


(a) The small image

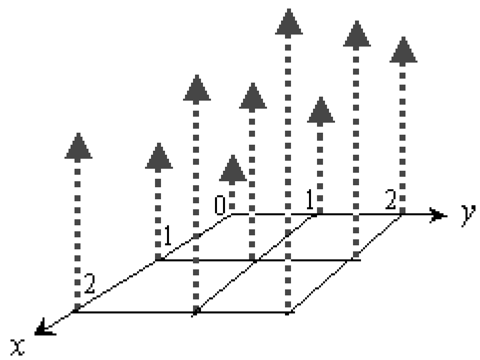


(b) The vertical vector field representing the small image of (a)

Fig. 1 A simple example of the vector field representing a small image

The curl source reverse is proposed as the reverse from the vertical field $\vec{I}$ to the virtual current density distribution (named the virtual curl source in this paper) imitating Equation (3). To achieve the curl source reverse, replace $\vec{B}$ in Equation (3) with $\vec{I}$:

$$\vec{C} = \nabla \times \vec{I} = \begin{vmatrix} \vec{i} & \vec{j} & \vec{k} \\ \frac{\partial}{\partial x} & \frac{\partial}{\partial y} & \frac{\partial}{\partial z} \\ I_x & I_y & I_z \end{vmatrix} =$$

$$\left(\frac{\partial I_z}{\partial y}-\frac{\partial I_y}{\partial z}\right)\vec{i}+\left(\frac{\partial I_x}{\partial z}-\frac{\partial I_z}{\partial x}\right)\vec{j}+\left(\frac{\partial I_y}{\partial x}-\frac{\partial I_x}{\partial y}\right)\vec{k} \quad (5)$$

where $\vec{C}$ is the virtual curl source; $\vec{i}$, $\vec{j}$ and $\vec{k}$ are the three unit vectors on the $x$, $y$ and $z$ coordinates respectively.

It is notable that the components of $\vec{I}$ on the $x$-coordinate and $y$-coordinate are both zero because it is defined as a vertical vector field. If Equation (4) and (5) are combined, the curl source reverse is as following:

$$\vec{C}=\begin{vmatrix} \vec{i} & \vec{j} & \vec{k} \\ \frac{\partial}{\partial x} & \frac{\partial}{\partial y} & \frac{\partial}{\partial z} \\ 0 & 0 & f(x,y) \end{vmatrix} = \frac{\partial f(x,y)}{\partial y}\vec{i}-\frac{\partial f(x,y)}{\partial x}\vec{j} \quad (6)$$

According to Equation (6), the result of curl source reverse is a vector field $\vec{C}(x,y)$ defined on the 2-D plane where the image $f(x,y)$ is defined.

Because $f(x,y)$ is a digital image, the two partial derivatives in Equation (6) should be estimated by discrete operators. In this paper, the Sobel operator is used for the estimation. The two templates for partial derivative estimation are shown in Fig. 2.

| | | |
|---|---|---|
| -1 | 0 | 1 |
| -2 | 0 | 2 |
| -1 | 0 | 1 |

The template to estimate the derivative on *x*-coordinate

| | | |
|---|---|---|
| 1 | 2 | 1 |
| 0 | 0 | 0 |
| -1 | -2 | -1 |

The template to estimate the derivative on *y*-coordinate

Fig. 2 The two templates of Sobel operator to estimate the gradient vector

According to the Sobel operator, for digital image $f(x,y)$, the two components of the virtual curl source are estimated as following:

$$C_x(x,y)=[f(x-1,y+1)-f(x-1,y-1)]+2[f(x,y+1)-f(x,y-1)]+[f(x+1,y+1)-f(x+1,y-1)]$$

$$C_y(x,y)=-[f(x+1,y-1)-f(x-1,y-1)]-2[f(x+1,y)-f(x-1,y)]-[f(x+1,y+1)-f(x-1,y+1)] \quad (7)$$

Equation (7) defines the operation of curl source reverse for digital images. The virtual curl source for an image is defined as a discrete vector field on the image plane, whose $x$ and $y$ components are defined in Equation (7). The properties of the virtual curl source are investigated experimentally in the next section.

## 3 The Spatial Properties of the Virtual Curl Source for Digital Images

Equation (6) indicates that for a vector in the virtual curl source, its component on the $x$-coordinate is the partial derivative of $f(x,y)$ with respect to $y$, and its component on the $y$-coordinate is the partial derivative with respect to $x$. On the other hand, it is well known that the gradient $\vec{G}$ of a field $f(x,y)$ also has the two partial derivatives as its components:

$$\vec{G}=\frac{\partial f(x,y)}{\partial x}\vec{i}+\frac{\partial f(x,y)}{\partial y}\vec{j} \quad (8)$$

It is indicated from Equation (6) and (8) that the virtual source obtained by the curl source reverse has direct relationship with the gradient field:

$$C_x(x,y)=G_y(x,y)$$
$$C_y(x,y)=-G_x(x,y) \quad (9)$$

Therefore, on any point in the image, the vector in the virtual source has the same magnitude of the gradient vector on that point, but their directions are different. According to Equation (9), the vector of $C$ is obtained by two steps: reflect the vector of $G$ across the line with the slope of 1.0, followed by another reflection across the $x$-axis. The relationship between a vector in the curl source and its corresponding gradient vector is shown in Fig. 3. Because the gradient is always taken as the feature of edges in the image, the virtual source obtained by the curl source reverse will also reflect structural feature of the image.

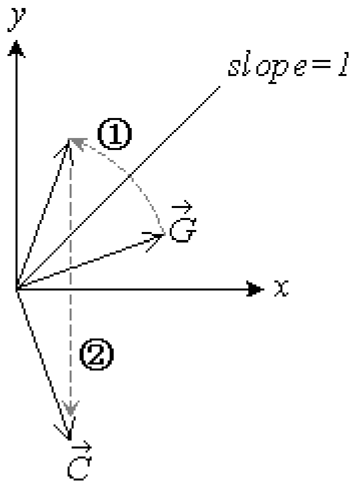


Fig. 3 The relationship between a vector in the curl source and its corresponding gradient vector

Experiments are carried out for a group of test images to reveal the basic properties of the virtual curl source. The curl source reverse is implemented in VC6.0 developing environment. The test images are of the size 32×32. The experimental results are shown in Fig. 4 to Fig. 8. The figures with the label (a) in Fig. 4 to Fig. 8 are the original test images. The figures with the label (b) in Fig. 4 to Fig. 8 are the magnitude distributions of the virtual curl source. The figures with the label (c) in Fig. 4 to Fig. 8 are the direction distributions of the virtual curl source.

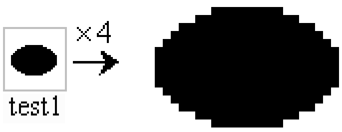


(a) The image *test1* (4 times of the original size on the right for a clear view)

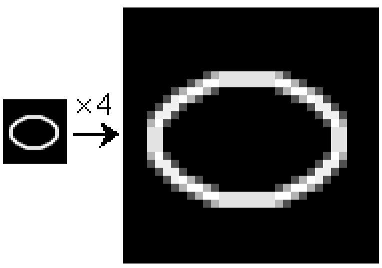


(b) The magnitude distribution of the virtual curl source of *test1* (4 times of the original size on the right for a clear view)

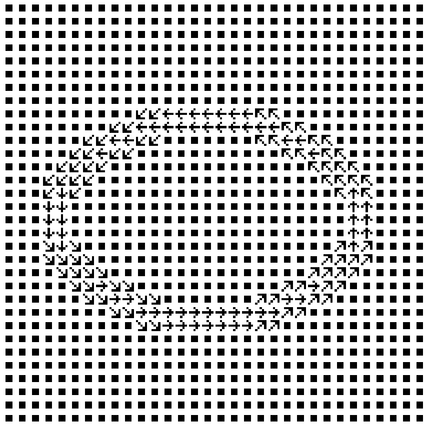

(c) The direction distribution of the virtual curl source of *test1*

Fig. 4 The result of curl source reverse for *test1*

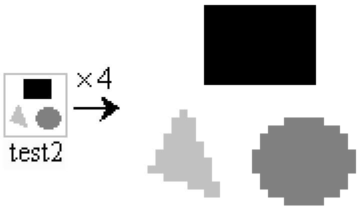


(a) The image *test2* (4 times of the original size on the right for a clear view)

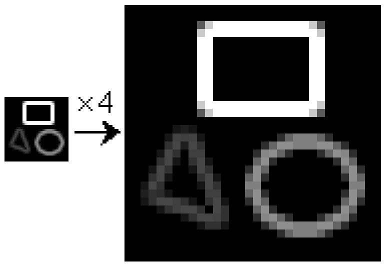


(b) The magnitude distribution of the virtual curl source of *test2* (4 times of the original size on the right for a clear view)

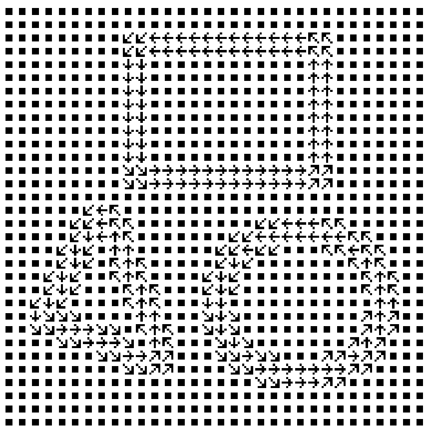

(c) The direction distribution of the virtual curl source of *test2*

Fig. 5 The result of curl source reverse for *test2*

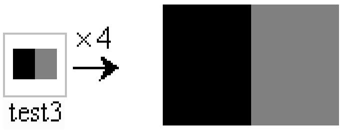


(a) The image *test3* (4 times of the original size on the right for a clear view)

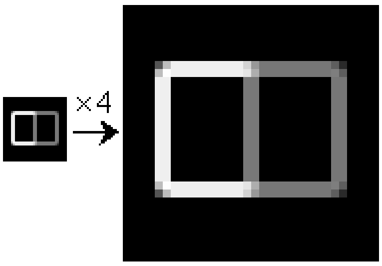


(b) The magnitude distribution of the virtual curl source of *test3* (4 times of the original size on the right for a clear view)

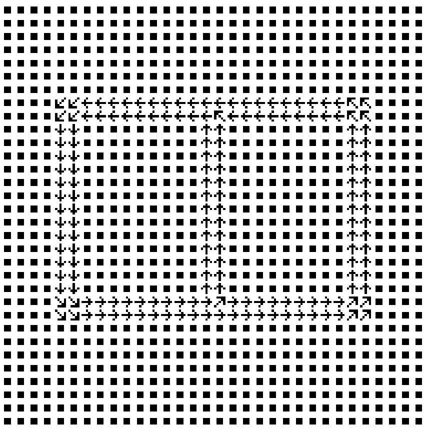

(c) The direction distribution of the virtual curl source of *test3*

Fig. 6 The result of curl source reverse for *test3*

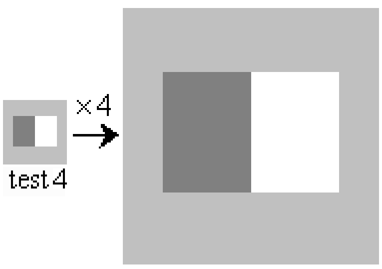


(a) The image *test4* (4 times of the original size on the right for a clear view)

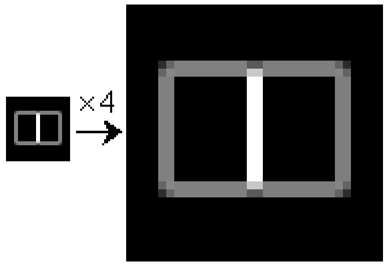


(b) The magnitude distribution of the virtual curl source of *test4* (4 times of the original size on the right for a clear view)

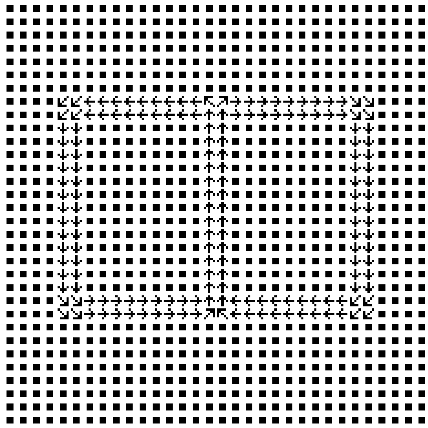

(c) The direction distribution of the virtual curl source of *test4*

Fig. 7 The result of curl source reverse for *test4*

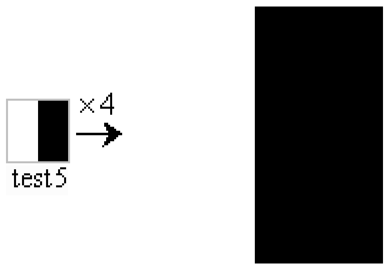


(a) The image *test5* (4 times of the original size on the right for a clear view)

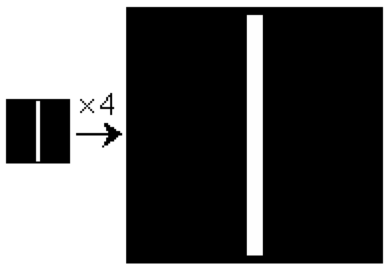


(b) The magnitude distribution of the virtual curl source of *test5* (4 times of the original size on the right for a clear view)

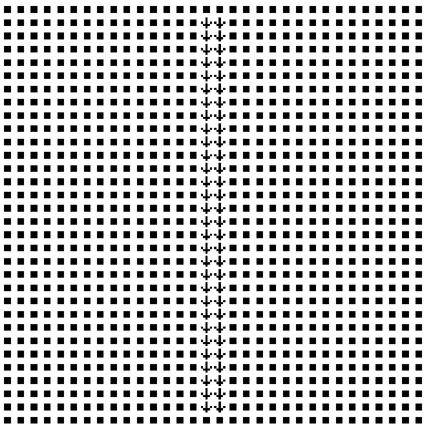

(c) The direction distribution of the virtual curl source of *test5*

Fig. 8 The result of curl source reverse for *test5*

The experimental results reveal the spatial properties of the virtual curl source. In the figures with the label (b) in Fig. 4 to Fig. 8, larger gray-scale values correspond to larger vector magnitudes. The figures with the label (b) in Fig. 4 to Fig. 8 show that the energy (i.e. non-zero values) in the virtual curl source concentrates near the region borders, where there is more complex structure than the other parts of the image [14,15]. This is because each vector in the virtual curl source has the same magnitude as the gradient vector at the same point, but their directions are different. This property of energy concentration in the magnitude distribution of the virtual curl source may be exploited in data compression, which is similar to the energy concentration of the 2-D Fourier transform in the frequency domain [16,17,18].

The direction distribution of the virtual curl source is shown in the figures with the label (c) in Fig. 4 to Fig. 8. The direction angle of each vector is visualized by discretizing into 8 discrete directions. The black dots in the figures with the label (c) in Fig. 4 to Fig. 8 indicate the positions of zero vectors. The representation and analysis of image structure is important for many image-processing tasks [19,20,21]. Experimental results indicate that the direction distribution of the virtual source has direct relationship with the image structure. In the figures with the label (c) in Fig. 4 to Fig. 8, the vectors in the virtual curl source have a rotating pattern as a whole, which rotate along the borders of the regions. For example, the curl vectors in Fig. 4(c) rotate anti-clockwise as a whole. On the other hand, the curl vectors in the source are zero within homogeneous regions.

Moreover, the rotating direction of the curl vectors as a whole has direct relationship with the gray-scale difference between adjacent regions. Experimental results indicate that when moving along the rotating direction indicated by the curl vectors, the region on the left hand has lower gray-scale than that on the right hand. Therefore, the spatial properties of the magnitude and direction distributions of the virtual curl source can be an effective representation of image structure, which may be exploited in further processing and analysis.

## 4 The Opposite Transform form the Virtual Curl Source to the Image

It is an important characteristic of a transform whether the transform is reversible. For the curl source reverse, the opposite transform from the virtual curl source to the original image is discussed in this section.

In physics, the continuous magnetic field $\vec{B}$ can be obtained from the distribution of the current density $\vec{J}$, which is well known as the Biot-Savart Law [12,13]:

$$\vec{B}(p) = \frac{\mu_0}{4\pi} \int_V \frac{\vec{J} \times \vec{r}}{r^3} dv \qquad (10)$$

where $\vec{B}(p)$ is the magnetic induction at the point *p*; $\vec{J}$ is the current density; $\vec{r}$ is the vector from the current density to the point *p*. The integral in Equation (10) is for the whole source space where there is current density distribution.

Imitating Equation (10), the restoration from the virtual source $\vec{C}(x, y)$ to the field $\vec{I}(x, y)$ (i.e. the image) is proposed. Because the virtual source and the gradient field are related by Equation (9), the proposed restoration method can also be a method for estimating the image from its gradient field.

Because $\vec{C}(x, y)$ is a vector field defined on a discrete 2-D plane, the restoration of the field $\vec{I}(x, y)$ should also use discrete operations, i.e. the integral in Equation (10) should be replaced by summation as following:

$$\vec{I}'(x, y) = K \cdot \sum_{j=1}^{H} \sum_{i=1}^{W} \frac{\vec{C}(i, j) \times \vec{r}_{(i,j)\to(x,y)}}{r^3_{(i,j)\to(x,y)}} \qquad (11)$$

where *K* is a constant; *H* and *W* are the height and width of the image respectively; $\vec{C}(i, j)$ is the virtual curl source; $\vec{I}'(x,y)$ is the restored field whose magnitude distribution corresponds to the image; $\vec{r}_{(i,j)\to(x,y)}$ is the vector from ($i$,$j$) to ($x$,$y$).

Because $\vec{r}_{(i,j)\to(x,y)}$ and $\vec{C}(x,y)$ are both vector fields on the 2-D plane, their components on $z$-coordinate are zero:

$$\begin{aligned} C_z &= 0 \\ r_z &= 0 \end{aligned} \tag{12}$$

Therefore, the cross product of $\vec{C}(x,y)$ and $\vec{r}_{(i,j)\to(x,y)}$ is as following:

$$\vec{C}\times\vec{r} = \begin{vmatrix} \vec{i} & \vec{j} & \vec{k} \\ C_x & C_y & C_z \\ r_x & r_y & r_z \end{vmatrix} = \begin{vmatrix} \vec{i} & \vec{j} & \vec{k} \\ C_x & C_y & 0 \\ r_x & r_y & 0 \end{vmatrix}$$

$$= (C_x r_y - C_y r_x)\vec{k} \tag{13}$$

where $r_x$ and $r_y$ are the two components of $\vec{r}_{(i,j)\to(x,y)}$ respectively. Combine Equation (11) and (13), the restoration of the field (i.e. the image) from the virtual curl source is as following:

$$\vec{I}'(x,y) = K \cdot \sum_{j=1}^{H}\sum_{i=1}^{W} \frac{(C_x(i,j)\cdot r_y - C_y(i,j)\cdot r_x)}{r^3_{(i,j)\to(x,y)}}\vec{k} \tag{14}$$

Because the virtual curl source is related to the gradient field of the image by Equation (9), the above restoration method is also a way to estimate the original image from its gradient field with the virtual curl source as an intermediary: first the gradient field can be transformed to $\vec{C}(x,y)$ according to Equation (9), then the image can be restored according to Equation (14).

Experiments of image restoration from the virtual curl source are carried out for a group of real world images. The experimental results are shown in Fig. 9 to Fig. 14. The figures with the label (a) in Fig. 9 to Fig. 14 are the visualization of the original data of the restored $\vec{I}'(x,y)$ 's magnitude distribution. The figures with the label (b) in Fig. 9 to Fig. 14 are the results after contrast enhancement of the corresponding original magnitudes. The figures with the label (c) in Fig. 9 to Fig. 14 are the original images for comparison.

(a) Visualization of *I'*(*x*,*y*)

(b) Result of contrast enhancement

(c) The original image of the boat

Fig. 9 The result of opposite transform from the virtual curl source to the boat image

(a) Visualization of *I'*(*x*,*y*)

(b) Result of contrast enhancement

(c) The original image of the bridge

Fig. 10 The result of opposite transform from the virtual curl source to the bridge image

(a) Visualization of $I'(x,y)$

(b) Result of contrast enhancement

(c) The original image of the house

Fig. 11 The result of opposite transform from the virtual curl source to the house image

(a) Visualization of $I'(x,y)$

(b) Result of contrast enhancement

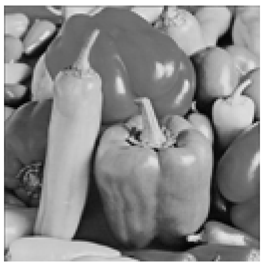

(c) The original image of the peppers

Fig. 12 The result of opposite transform from the virtual curl source to the peppers image

(a) Visualization of $I'(x,y)$

(b) Result of contrast enhancement

(c) The original image of the cameraman

Fig. 13 The result of opposite transform from the virtual curl source to the cameraman image

(a) Visualization of $I'(x,y)$

(b) Result of contrast enhancement

(c) The original image of the broadcaster

Fig. 14 The result of opposite transform from the virtual curl source to the broadcaster image

The results indicate that the restored images can be good approximations of the original image for visual understanding, but there are differences between the restored and original images. Although the transform for continuous field defined by Equation (3) and (10) are reversible, the curl source reverse for digital images defined by Equation (7) and (14) includes operations of discretization, which introduces data errors into the restored results. Therefore, the proposed transform of curl source reverse is not strictly reversible, but the opposite transform from the virtual curl source to the image just provides acceptable results for visual perception.

## 5 Conclusion

In this paper, the curl source reverse is presented for digital images. The virtual curl source is estimated imitating the magneto-static field as a novel representation of image structure. The experimental results for test images indicate that the virtual curl source can be an effective representation of image structure for further analysis. Moreover, the visually acceptable approximation for the original images can be derived from the virtual curl source, based on which a method of image estimation and restoration from its gradient field is proposed. Experimental results for real world images prove the effectiveness of the proposed method. The experiments also indicate that in the representation by the virtual curl source the energy concentrates on the region borders, which may be exploited in image data compression. Further research will investigate the application of the curl source reverse in other image processing applications. It will also be investigated to remove the data errors caused by discretization in the transform process so that the opposite transform from the virtual curl source to the image can have the quality similar to those strictly reversible transforms.

*References:*


[1] YuJin Zhang. *Image Engineering*: *Image Processing* (*2nd Edition*), TUP Press, Beijing, China, 2006.

[2] R.N. Bracewell, *The Fourier Transform and Its Applications* (Series in Electrical Engineering), McGraw-Hill Book Company, New York, 1986.

[3] S. Mallat, A theory for multiresolution signal decomposition: The wavelet representation, *IEEE Pat. Anal. Mach. Intell.*, Vol. 11, No. 7, pp. 674-693, July 1989.

[4] D. J. Hurley, M. S. Nixon and J. N. Carter, Force field feature extraction for ear biometrics, *Computer Vision and Image Understanding*, Vol. 98, No. 3, 2005, pp. 491-512.

[5] X. D. Zhuang and N. E. Mastorakis, The Curling Vector Field Transform of Gray-Scale Images: A Magneto-Static Inspired Approach, *WSEAS Transactions on Computers*, Issue 3, Vol. 7, 2008, pp. 147-153.

[6] G. Abdel-Hamid and Y. H. Yang, Multiscale Skeletonization: An electrostatic field-based approach, *Proc. IEEE Int. Conference on Image Processing*, Vol. 1, 1994, pp. 949-953.

[7] Luo, B., Cross, A. D. and Hancock, E. R., Corner Detection Via Topographic Analysis of Vector Potential, *Pattern Recognition Letters*, Vol. 20, No. 6, 1999, pp. 635-650.

[8] Andrew D. J. Cross and Edwin R. Hancock, Scale-space vector field for feature analysis, *Proceedings of the IEEE Computer Society Conference on Computer Vision and Pattern Recognition*, 1997, pp. 738-743.

[9] K. Wu and M. D. Levine, 3D part segmentation: A new physics-based approach, *IEEE International symposium on Computer Vision*, 1995, pp. 311-316.

[10] N. Ahuja and J. H. Chuang, Shape Representation Using a Generalized Potential Field Model, *IEEE Transactions PAMI*, Vol. 19, No. 2, 1997, pp. 169-176.

[11] T. Grogorishin, G. Abdel-Hamid and Y.H. Yang, Skeletonization: An Electrostatic Field-Based Approach, *Pattern Analysis and Application*, Vol. 1, No. 3, 1996, pp. 163-177.

[12] P. Hammond, *Electromagnetism for Engineers*: *An Introductory Course*, Oxford University Press, USA, forth edition, 1997.

[13] I. S. Grant and W. R. Phillips, *Electromagnetism*, John Wiley & Sons, second edition, 1990.

[14] X. Zhuang, N. E. Mastorakis, The Local Fuzzy Fractal Dimension as a Feature of Local Complexity for Digital Images and Signals, *WSEAS transactions on Computers*, Issue 11, Vol. 4, November 2005, pp. 1459-1469.

[15] Michiharu Niimi, Hideki Noda and Eiji Kawaguchi, An image embedding in image by a complexity based region segmentation method, *Proceedings of 1997 International Conference on Image Processing*, Vol.3, 1997, pp. 74-77.

[16] Andrew B. Watson, Image Compression Using the Discrete Cosine Transform, *Mathematica Journal*, 4(1), 1994, pp. 81-88

[17] Ahmed, N., T. Natarajan, and K. R. Rao, On image processing and a discrete cosine transform. *IEEE Transactions on Computers*, C-23(1), 1974, pp. 90-93.

[18] Wallace G., The JPEG still picture compression standard, *Communications of the ACM*, 34(4), 1991, pp. 30-44.

[19] L. M. J. Florack, *Image Structure*, (volume 10 of Computational Imaging and Vision Series), Kluwer Academic Publishers, Dordrecht, 1997.

[20] X. Zhuang, N. E. Mastorakis, Image Processing with the Artificial Swarm Intelligence, *WSEAS transactions on Computers*, Issue 4, Vol. 4, April 2005, pp. 333-341.

[21] I. V. Gribkov, P. P. Koltsov, N. V. Kotovich, A. A. Kravchenko, A. S. Koutsaev, A. S. Osipov, A. V. Zakharov, Testing of Image Segmentation Methods, *WSEAS Transactions on Signal Processing*, Issue 8, Vol. 4, August 2008, pp. 494-503